Specific DNA Recognition by the Type II Restriction Endonuclease *Mun*I: The Effect of pH[†]

Ihtshamul Haq,[‡,§] Ronan O'Brien,[‡] Arunas Lagunavicius,[||] Virginijus Siksnys,[||] and John E. Ladbury*[,‡]

Department of Biochemistry and Molecular Biology, University College London, Darwin Building, Gower Street, London, WC1E 6BT, U.K., and Institute of Biotechnology, Graiciuno 8, Vilnius 2028, Lithuania

Received June 27, 2001; Revised Manuscript Received September 17, 2001

ABSTRACT: To investigate the effect of pH on sequence-specific binding, a thermodynamic characterization of the interaction of the protein *Mun*I with a specific, and a nonspecific, oligonucleotide was performed. *Mun*I is a type II restriction endonuclease which is able to bind specifically, but loses its enzymatic activity in the absence of magnesium ions. Comparison of the specific and nonspecific interactions at 10 and 25 °C shows that the latter is accompanied by a small change in enthalpy, and a negligible change in constant pressure heat capacity. On going through the pH range 5.75−9.0 at 25 °C, the affinity of specific complex formation is reduced by 20-fold. The interaction is accompanied by the protonation of groups assumed to be on the protein. Based on the simplest model that will fit the data, two distinct protonation events are observed. At low pH, two groups per protein molecule undergo protonation with a pK_a of 6.0 and 6.9 in the free and bound forms, respectively. At high pH, a further independent protonation occurs involving two groups with pK_a values of 8.9 and approximately 10.7 in the free and bound forms, respectively. The change in heat capacity ranges from −2.7 to −1.7 kJ mol^{-1} K^{-1} in going from pH 6.5 to 8.5. This range of variation of change in heat capacity can be accounted for by the effects of protonation of the interacting molecules. The change in heat capacity, calculated from surface area burial using a previously established relationship (1.15 kJ mol^{-1} K^{-1}), does not correlate well with the experimentally determined values.

The complex functioning and regulation of genetic material is mediated by, and reliant upon, noncovalent interactions between nucleic acids and proteins. In order for genetic regulation to occur successfully, it is necessary for a protein to recognize a specific base pair sequence in DNA and correctly distinguish this target sequence from all other potential binding sites on the DNA lattice. The extent of specificity in the DNA−protein interaction varies, from permissive to extremely stringent, and is dependent on the exact function of the protein.

Restriction endonucleases are an important class of proteins that exhibit extreme specificity for their targets. This is necessary because these enzymes must efficiently cleave small, 4−8 base pair, recognition sites on foreign DNA while avoiding potentially lethal cleavage of the host DNA containing sites that differ by perhaps only 1 base pair. This property makes restriction endonucleases ideal candidates for probing the determinants of sequence-specific DNA recognition using structural and biophysical approaches. To cleave phosphodiester bonds in DNA, type II restriction endonucleases require Mg^{2+} ions as a cofactor (*1*). However in the absence of magnesium, some of these proteins (for example, *Eco*RI, *Rsr*I, and *Bam*HI) retain their ability to specifically recognize the cognate DNA sequence, and bind to it preferentially, without exhibiting catalytic activity (*2*−*4*). Other restriction endonucleases (for example, *Eco*RV, *Taq*I, and *Cfr*9I) bind with equal affinity to cognate and noncognate DNA targets in the absence of Mg^{2+} (*5*−*7*). These characteristics allow restriction endonucleases to be used as model systems for examining both specific and nonspecific DNA binding.

To extend our understanding of sequence-specific recognition, here we investigate the thermodynamics of *Mun*I binding to DNA. *Mun*I is a type II restriction endonuclease, which is able to bind specifically to, but loses its ability to cleave, its cognate sequence (C$^{\downarrow}$AATTG) in the absence of Mg^{2+} (*8*). Active site carboxylate residues have already been demonstrated as being important in modulating binding specificity (*9*). Any DNA−protein interaction in which the protein possesses ionizable residues, or makes electrostatic contacts with the target binding site, will be profoundly affected by pH; however, the *Mun*I−DNA interaction provides an opportunity to investigate a more complex multiple protonation event over a limited pH range on a small, stable protein and short oligonucleotide. We adopted isothermal titration calorimetry (ITC)[1] to measure the effect of pH on the binding of *Mun*I to DNA duplexes containing

[†] This work was supported by a Wellcome Trust Biomedical Research Collaboration Grant for J.E.L and V.S. J.E.L. is a Wellcome Trust Senior Research Fellow. V.S. is supported in part by a Howard Hughes Medical Institute International Scholarship Grant.

* Corresponding author. Tel: +44 (0)20 7679 7012; Fax: +44 (0)20 7679 7193; E-mail: j.ladbury@biochem.ucl.ac.uk.

[‡] University College London.

[§] Current address: Centre for Chemical Biology, Krebs Institute for Biomolecular Science, Department of Chemistry, University of Sheffield, Sheffield, S3 7HF, U.K.

[||] Institute of Biotechnology.

[1] Abbreviations: ITC, isothermal titration calorimeter; ΔC_p, constant pressure change in heat capacity; SP, specific; NSP, nonspecific; ΔA_p, change in polar surface area; ΔA_{np}, change in nonpolar surface area.

10.1021/bi0113566 CCC: $20.00
Published on Web 11/15/2001

a single, specific recognition site [d(GCCAATTGGC)$_2$] and an equivalent nonspecific oligonucleotide [d(GCCACGTGGC)$_2$] in order to evaluate linked protonation effects in the binding site. In addition, we also explored the change in heat capacity (ΔC_p) as a function of pH. We also demonstrate that the variation in ΔC_p observed at different pH values can, at least in part, be attributed to protonation effects.

MATERIALS AND METHODS

Protein Purification. Purification of the *Mun*I protein was carried out as previously described (*9*, *10*). Analysis of the purified protein by SDS−PAGE showed that the enzyme was >99% homogeneous. Stock solutions of protein were stored at −20 °C in a buffer containing 10 mM Tris/HCl, 100 mM KCl, 1 mM Na$_2$EDTA, 1 mM DTT, and 50% glycerol, pH 7.5. Prior to use in binding studies, 1 mL aliquots of the stock protein were dialyzed against 2 L of the appropriate experimental buffer for 24 h using dialysis tubing with a 3000 molecular weight cutoff. Protein solutions were quantified spectrophotometrically using an extinction coefficient (calculated from amino acid composition) at 280 nm for monomers of 45 720 M^{-1} cm^{-1}. Throughout this paper, protein concentrations are expressed in terms of dimers. The stability of the protein was assessed calorimetrically, and no evidence of denaturation in the temperature or pH range studied was observed.

DNA Oligonucleotides. The two DNA duplexes used in this study, d(GCCAATTGGC)$_2$ (specific: termed SP) and d(GCCACGTGGC)$_2$ (nonspecific: termed NSP), were purchased from the Oswel DNA Service (University of Southampton, U.K.) as 10 μM preparations. The oligonucleotides were purified by the manufacturer using HPLC to >99.5% purity. DNA solutions were prepared by dissolving the lyophilized 10-mers in the relevant buffer and then dialyzing for 24 h against 2 L of the same buffer using 500 molecular weight cutoff tubing. Following dialysis, DNA solutions were heated to 98 °C for 5 min and then allowed to slow-cool to room temperature prior to storage at 4 °C. UV melts were carried out on each of the duplexes in a buffer containing 10 mM MOPS, 200 mM NaCl, 1 mM Na$_2$EDTA, pH 7.5. From these experiments, it was determined that the SP duplex had a T_m of 46.3 °C and melting-induced hyperchromism of 24.7%. The NSP duplex had a T_m of 58.7 °C and a hyperchromism of 22.2%. These data were used to apply a correction to single-strand extinction coefficients calculated from a consideration of nearest-neighbor interactions (*11*). The corrected extinction coefficients used in this study for the quantification of DNA oligomers are as follows: $\epsilon_{260} = 1.48 \times 10^5$ M(duplex)$^{-1}$ cm^{-1} for SP and 1.47×10^5 M(duplex)$^{-1}$ cm^{-1} for NSP.

Isothermal Titration Calorimetry (ITC). Equilibrium binding studies designed to examine the interaction of *Mun*I with SP and NSP DNA duplexes were carried out using the isothermal titration module of a MicroCal MCS (MicroCal Inc., Amherst, MA) calorimeter. Data acquisition and analysis were carried out using ORIGIN 2.9 software (MicroCal LLC., Northampton, MA). In a typical experiment, titrations were set up such that up to 19, 15 μL injections of 0.3 mM (duplex) SP or NSP were made into *Mun*I in the sample cell at 30 μM at 300 s time intervals. An initial injection of 3 μL was also made to expel any air bubbles from the syringe needle and also to negate the effects of any slight ligand−macromolecule diffusion that may have occurred during thermal equilibration.

ITC protocols have been comprehensively described elsewhere (*12*−*14*). It is necessary to carry out control experiments where the contributions of heats of dilution to the overall observed enthalpy are determined. This involved three titations: (1) where oligonucleotide solution, at the same concentration as that used in the binding experiment, is injected into the buffer alone, (2) where buffer is injected into 30 μM protein, and (3) where buffer is injected into buffer. These background heats were found to be constant, indicating there is no dissociation of the protein dimer or of the duplex DNA upon dilution. A corrected binding enthalpy was obtained by subtracting the heats of dilution from the observed binding enthalpy and summing the result with a small contribution from the buffer into buffer titration. Binding enthalpies are determined directly from the primary data, and binding constants and stoichiometries were obtained by fitting the corrected isotherms to a model, incorporated into the ORIGIN software, that assumes a single set of identical binding sites.

Determination of the pH Dependence of Interaction. ITC was used to examine the effects of pH on the equilibrium binding constant at 25 °C. Titrations were carried out on samples of *Mun*I and SP that had been dialyzed in a triple buffer system with a pH range of 5.5−9.0. An identical triple buffer was prepared for all the different ITC experiments at various pH values; this buffer contained 25 mM MES, 25 mM sodium acetate, 50 mM Tris/HCl, 150 mM NaCl, and 1 mM Na$_2$EDTA; the pH was then adjusted to the required value with small additions of acid or base (*15*). The purpose of choosing this buffer system was to maintain constant ionic strength across the pH range examined.

In a separate second set of experiments, we examined the effect of ΔH_{ion} (ionization enthalpy of the buffer) on ΔH_{obs}. Here we measured the enthalpy at a fixed pH using different buffers. The buffer system used here was one of the following at a concentration of 10 mM (pH 6.5 = cacodylate, phosphate, MES, PIPES; pH 7.5 = MOPS, HEPES, phosphate, BES; pH 8.5 = Tris, tricine, bicine, TAPS), 150 mM NaCl, 1 mM Na$_2$EDTA. The values for ΔH_{ion} for each buffer were taken from standard literature values (*16*).

The protein is considered to be a dimer throughout the pH range adopted in these experiments based on previously published data. These indicate that within the pH range 6.0−9.0 the cleavage patterns of plasmid DNA under steady-state conditions exhibited product burst kinetics. The burst amplitude, which actually reflects the concentration of enzyme active sites, was equal to the concentration of the enzyme dimers at all pH values. These data indicate that *Mun*I is a stable dimer throughout the pH range 6.0−9.0 (*17*).

Measurement of Heat Capacity. The binding-induced heat capacity change for the *Mun*I−SP interaction was determined at three pH values. This was achieved by dialyzing protein and DNA stock solutions in one of the following buffers: 10 mM MES, 200 mM NaCl, 1 mM Na$_2$EDTA, pH 6.5; 10 mM MOPS, 200 mM NaCl, 1 mM Na$_2$EDTA, pH 7.5; or 10 mM TAPS, 200 mM NaCl, 1 mM Na$_2$EDTA, pH 8.5. ITC titrations were performed as described above between 10 and 30 °C. Corrected binding enthalpies were then plotted

against the recorded temperature; the slope of the linear least-squares fit of the data yielded the heat capacity change.

Calculation of Solvent-Accessible Surface Areas. Solvent-accessible surface areas were generated from atomic coordinates for the X-ray structure of the D83A mutant *Mun*I−SP complex [(*18*); PDB entry: 1D02; NDB entry: pd0151) using an analytical function within the GRASP 1.3.6 software (*19*). This procedure uses Leonard−Jones atomic radii and a probe radius of 1.4 Å. Surfaces of carbon, carbon-bound hydrogen, and phosphorus atoms were defined as nonpolar (hydrophobic), whereas those of all other atoms were defined as polar (hydrophilic). Calculation of the nonpolar (hydrophobic) and polar (hydrophilic) surface areas was carried out for the complex, the separated individual components, i.e., the protein dimer and DNA duplex, and canonical B-DNA of the sequence d(GCCAATTGGC)$_2$ generated using the GENHELIX-2 program. The change in surface area upon binding, ΔA, is the difference between the area of the complex and the summed surface areas of the protein-free DNA duplex and the protein dimer separated from the complex. Predictive algorithms that relate ΔC_p to changes in solvent-accessible surface area have been developed empirically using data from the heats of transfer of small hydrocarbons and protein folding−unfolding equilibria (*20*). The theoretical change in heat capacity was calculated using the relationship:

$$\Delta C_p = [0.32(\pm 0.04)\Delta A_{np} - 0.14(\pm 0.04)\Delta A_p]\ 4.18\ \text{J mol}^{-1}\ \text{K}^{-1}$$

where ΔA_{np} and ΔA_p are the binding-induced changes in nonpolar and polar surface area, in units of Å^2, respectively (*20*).

RESULTS

Specificity of MunI−DNA Complex Formation. The binding of *Mun*I to DNA oligonucleotides containing the specific recognition site for this protein (d[GCCAATTGGC]$_2$ = SP) and an equivalent DNA lacking the specific recognition site (d[GCCACGTGGC]$_2$ = NSP) was investigated using ITC. Figure 1 (left panel) shows sample raw calorimetric data for the *Mun*I−SP interaction at 19.5 °C in a pH 6.5 MES buffer with 200 mM NaCl. Integration of the peaks with respect to time, and conversion to a per mole basis, produces the binding isotherm shown in Figure 1 (right panel). Measured and calculated thermodynamic parameters for the binding of *Mun*I to the SP oligonucleotide under a variety of pH and buffer-type conditions are collated in Table 1.

Figure 2 shows the results obtained for the titration of NSP into *Mun*I. These experiments were carried out at pH 6.5 in a buffer containing 200 mM NaCl and at two temperatures (10 and 25 °C). These data show that there is little or no difference between the binding experiment and the control experiment where DNA was injected into buffer alone. Despite the fact that gel shift assays and CD experiments have shown previously that *Mun*I does bind to DNA sequences lacking a cognate recognition site at pH 6.5 (*8*), we observed negligible heat of binding in the ITC experiments. Thus, the interaction of the protein and NSP at the two temperatures studied has a near zero enthalpy of binding, and is thus governed by a favorable entropic contribution to

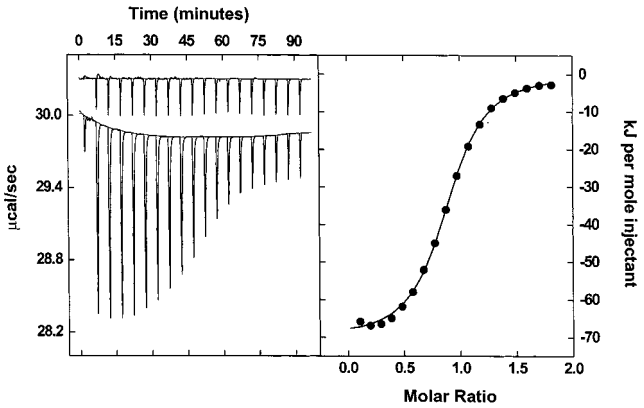

FIGURE 1: Sample raw data for the titration of SP into *Mun*I at 19.5 °C. In the left panel, the peaks in the lower data set show the heat produced by 15 μL serial injections of 0.3 mM(duplex) SP oligonucleotide into 1.13 mL of 30 μM *Mun*I contained in the sample cell of the calorimeter. Integration of these peaks produces the binding isotherm shown in the right panel (closed circles). The control dilution experiment is shown in the left panel, upper data set, where an identical DNA solution is injected into 1.13 mL of 10 mM MES, 200 mM NaCl, 1 mM Na_2EDTA, pH 6.5, buffer. Integration of these peaks after subtraction of the heats of diliution is shown in the right panel. The points are fitted to a model for a single independent binding site (see Materials and Methods).

the change in free energy. This is consistent with the previously reported interactions of *cro* repressor (*21*) and *trp* repressor (*22*) with noncognate oligonucleotides. Performing the binding of *Mun*I to NSP at two temperatures shows that this interaction is accompanied by zero ΔC_p. This is a common feature of nonspecific interactions between proteins and DNA (*13*, *21*−*23*).

pH Dependence of K_{obs}. Having demonstrated the distinct thermodynamic characteristics of specific complex formation, we investigated the role of pH in this interaction. Thermodynamic parameters for *Mun*I−SP binding as a function of pH in the range 5.5−9.0 were determined from ITC experiments and are summarized in Table 1. A triple buffer system was used throughout in order to eliminate variations in K_{obs} due to differences in the ionic strength of different buffers at different pH values. Figure 3 shows that there is a significant dependence of K_{obs} on the pH. In attempting to interpret any trends in thermodynamic measurements, a model has to be adopted and tested against the data. Here we demonstrate that the simplest model relating the K_{obs} to pH is not entirely appropriate, and thus invoke a more complex model to describe the data obtained.

The simplest possible model that describes a proton-linked binding event involves a single change in proton affinity (i.e., pK_a) of an ionizable group. The K_{obs} at any pH for this model can be determined from eq 1 (*24*, *25*):

$$K_{obs} = K_{int}\frac{1 + 10^{(pK_a)_b - pH}}{1 + 10^{(pK_a)_f - pH}} \quad (1)$$

where K_{obs} is the observed binding constant, K_{int} is the binding constant in the absence of any protonation effects, and $(pK_a)_f$ and $(pK_a)_b$ are the pK_a's of the free and bound forms of the protonated group, respectively. A plot of K_{obs} at any pH for a single change in proton affinity would produce a simple sigmoidal curve (*25*). Figures 3 and 4 suggest that this model is not appropriate for the herein

Table 1: Calorimetrically Measured Thermodynamic Parameters for the *Mun*I−SP Interaction as a Function of pH and Buffer Type at 25 °C[a]

buffer[b]	[NaCl] mM	pH	ΔH_{obs}[c] (kJ mol^{-1})	K_{obs}[d] ($\times 10^5$ M^{-1})	n[d]	ΔG_{obs} (kJ mol^{-1})	$T\Delta S$ (kJ mol^{-1} K^{-1})
triple	150	5.5	−70.9 ± 1.6	32.0 ± 0.6	0.9	−37.2	−33.7
triple	150	6.0	−96.9 ± 2.1	21.4 ± 0.4	0.9	−36.2	−60.7
triple	150	6.5	−84.3 ± 2.3	13.4 ± 0.4	1.0	−35.0	−49.3
triple	150	7.0	−62.2 ± 2.6	8.6 ± 0.3	1.1	−34.0	−28.2
triple	150	7.5	−56.1 ± 1.8	6.2 ± 0.5	0.9	−33.1	−23.0
triple	150	8.0	−27.1 ± 1.5	5.6 ± 0.6	0.9	−32.8	+5.7
triple	150	8.5	−24.6 ± 1.7	3.3 ± 0.2	1.2	−31.5	+6.9
triple	150	9.0	−21.7 ± 1.6	1.6 ± 0.4	1.1	−29.7	+8.0
MES[e]	200	5.75	−90.3 ± 4.6	121	0.9	−40.4	−50.1
Bistris[e]	200	5.75	−77.3 ± 8.6	37.8	1.0	−37.5	−39.8
acetate[e]	200	5.7.5	−56.7 ± 2.3	268	0.9	−42.4	−14.3
cacodylate	200	6.5	−101 ± 2.8	11.3 ± 0.2	1.1	−34.6	−66.4
phosphate	200	6.5	−91.1 ± 2.5	37.9 ± 0.1	1.0	−37.5	−53.6
PIPES	200	6.5	−74.2 ± 2.7	54.4 ± 0.3	1.2	−38.4	−35.8
MES	200	6.5	−80.0 ± 2.6	10.1 ± 0.2	0.9	−34.3	−45.7
phosphate	200	7.5	−75.2 ± 2.1	8.8 ± 0.5	1.3	−34.0	−41.2
HEPES	200	7.5	−66.4 ± 1.8	9.0 ± 0.4	1.0	−34.0	−32.4
MOPS	200	7.5	−64.0 ± 1.9	7.2 ± 0.3	0.9	−33.4	−30.6
BES	200	7.5	−62.7 ± 2.3	11.0 ± 0.6	0.9	−34.5	−28.2
imidazole	200	8.0	−32.5 ± 0.9	10.6 ± 1.7	0.8	−34.4	+1.9
Tricine	200	8.0	−35.8 ± 0.4	6.4 ± 0.4	0.8	−33.1	−2.7
Tris	200	8.0	−21.5 ± 0.4	7.7 ± 0.8	0.8	−33.6	+12.1
HEPES	200	8.0	−40.6 ± 0.8	4.5 ± 0.4	0.9	−32.2	−8.4
Bicine	200	8.5	−58.0 ± 2.0	4.2 ± 0.7	0.9	−32.1	−25.9
Tricine	200	8.5	−51.0 ± 1.6	1.5 ± 0.6	0.8	−29.6	−21.4
TAPS	200	8.5	−23.5 ± 1.8	5.4 ± 0.4	0.9	−32.7	+9.2
Tris/HCl	200	8.5	−6.8 ± 2.1	7.2 ± 0.8	0.9	−33.4	+26.6

[a] All binding data reported are based on at least two individual ITC experiments. [b] In all cases, buffer salts were used at concentrations of 10 mM except for the pH dependence of K_{obs} where a triple buffer was used (see Materials Methods). [c] Binding enthalpy determined directly using ITC. From these experimentally determined parameters, the free energy of binding (ΔG) and the entropy change (ΔS) can be determined using the standard thermodynamic relationship: $\Delta G = -RT \ln K_{obs} = \Delta H - T\Delta S$. [d] The equilibrium binding constant and reaction stoichiometry were obtained from ITC experiments by fitting corrected binding isotherms, using nonlinear least-squares procedures, to a model that assumes a single set of identical binding sites. [e] At pH 5.75, there is some evidence for weak nonspecific binding accompanying the specific binding event. Fitting these data to the two distinct binding events gives a distorted, but large error in the value of the K_{obs} due to the inability to accurately fit the nonspecific binding. No such events were observed in the triple buffer system.

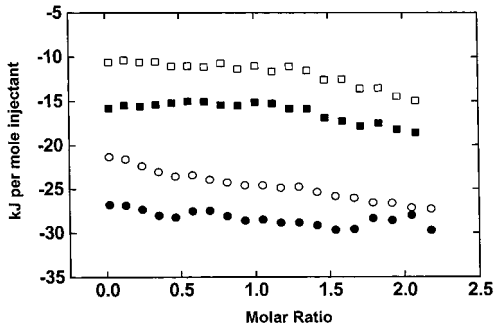

FIGURE 2: Calorimetric titrations of NSP oligonucleotide into *Mun*I dimers. These experiments were carried out in a buffer containing 10 mM MES, 200 mM NaCl, 1 mM Na_2EDTA, pH 6.5, and at two temperatures: 10 and 25 °C (circles and squares, respectively). In each case, the concentration of NSP oligonucleotide used was 0.3 mM(duplex), and each point represents an injection of 15 μL. The protein in the cell was at 30 μM. The closed symbols are data for the titration of DNA into protein whereas the open symbols show the results when protein in the cell is replaced by the buffer.

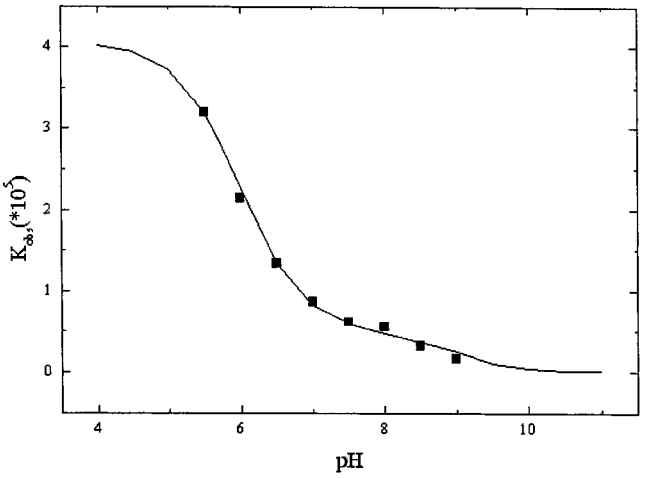

FIGURE 3: Variation of the equilibrium binding constant (K_{obs}) for the SP−*Mun*I interaction as a function of pH at 25 °C. For these experiments, a triple buffer system was used that contained 25 mM sodium acetate, 25 mM MES, 50 mM Tris/HCl, 150 mM NaCl, and 1 mM Na_2EDTA. The pH was adjusted using small additions of acid or base as necessary to achieve the desired pH. The data up to pH 8 were used to obtain initial parameters to improve the reliability of the global fit shown.

reported data since the curve has two distinct inflections. This suggests that protonation occurs over more than one pK_a range.

The simplest model which best fit our data over the entire pH range studied is based on protonation of ionizable groups within two distinct pK_a ranges. This model can be represented by the equilibrium Scheme 1 where M is the protein (since *Mun*I is a dimer in the free and bound states, M corresponds to two protein molecules; i.e., the dimerization constant is sufficiently high that the respective concentrations of monomer and dimer are unaffected under the conditions adopted in this work). D is the DNA (ligand), and H^+ is the proton.

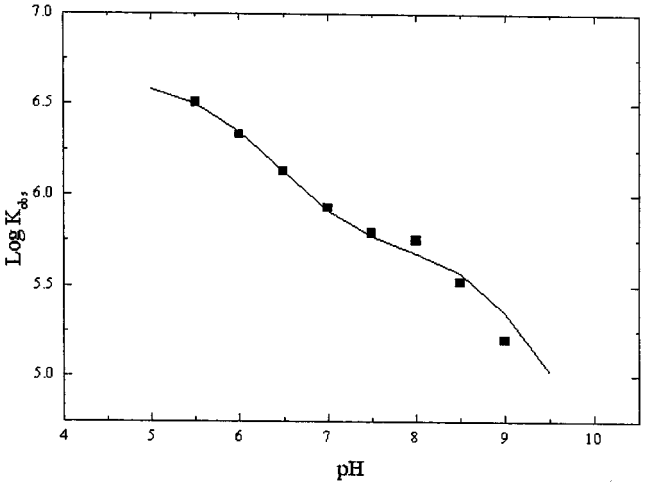

FIGURE 4: Graph of log K_{obs} against pH. Data are derived from those from Table 1 in the triple buffer shown in Figure 3. The solid line is the line of best fit to the data to the two-event model using eq 2. The best-fit parameters are indicated in the text.

Scheme 1

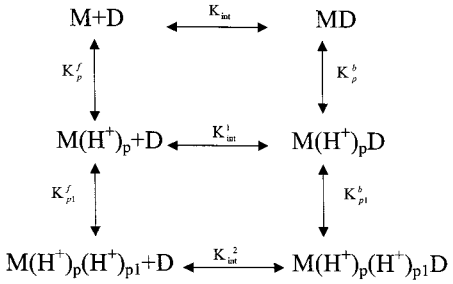

The superscripts *b* and *f* refer to the bound and free forms, respectively, while the subscripts *p* and *p*1 identify the two separate events at low and high pH, respectively. K^1_{int} is the binding constant of the protonated state of the protein to the ligand at low pH. K^2_{int} is the binding constant for the interaction between the protein and SP at high pH. This model describes a situation whereby at a given pH a group (or groups with identical pK_a values) experiences a protonation event(s) dependent on the pK_a of the group. Here we define a group as a chemical moiety on the protein which can be protonated (i.e., in the pH range considered, we make the assumption that the DNA does not undergo protonation). It is further assumed in this model that the different pK_a ranges which influence the protonation events of the group (or groups) are sufficiently different so as not to impinge on one another.

For this model, the data for K_{obs} as a function of pH are used to determine the values of the pK_a's of the protonated groups by fitting to eq 2 (*24*, *25*):

$$K_{obs} = K_{int}\frac{1 + 10^{(pK_a)_b - pH} + 10^{pH-(pK_a)_{b1}}}{1 + 10^{(pK_a)_f - pH} + 10^{pH-(pK_a)_{f1}}} \qquad (2)$$

where $(pK_a)_{b1}$ and $(pK_a)_{f1}$ are the pK's of the free and bound forms of the second ionization event. These are shown directly in Figure 3 (and by using log K_{obs} in Figure 4). The appropriateness of this simplification is discussed below. From a global fit using this model and assuming independence of events in the two pK_a ranges, we obtain the following ranges of pK_a's: $(pK_a)_f = 6.0 \pm 0.05$; $(pK_a)_b = 6.9 \pm 0.05$; $(pK_a)_{f1} = 8.9 \pm 0.05$; $(pK_a)_{b1} = 10.7 \pm 1.0$; and $K^1_{int} = (5.1 \pm 0.31) \times 10^5\ M^{-1}$. The error margins on the data quoted above correspond to those obtained from a Monte Carlo simulation of this data set in which a randomized error was introduced based on a maximum error in the determination of K_{obs} of $1.0 \times 10^5\ M^{-1}$. This assumed error in K_{obs} is based on the average error experienced on repetition of ITC experiments and is consistent with error margins observed in previously reported data (see, for example, *26*). Clearly, the pK_a value above 10 is outside the experimentally measured pH range, and as a result should be taken as an approximate value.

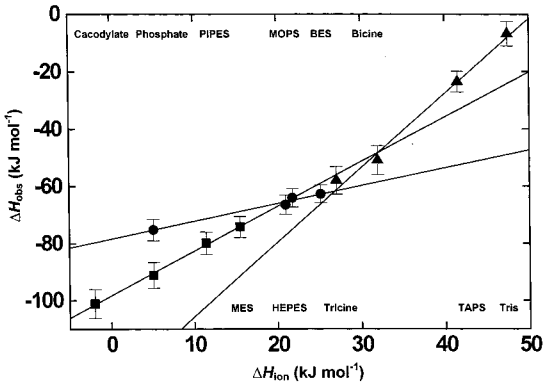

FIGURE 5: Binding enthalpies for the binding of SP to *Mun*I at pH 6.5, 7.5, and 8.5 as a function of the ionization enthalpy (ΔH_{ion}) of the buffer. The solution conditions in these experiments were 10 mM buffer, 150 mM NaCl, and 1 mM Na_2EDTA and 25 °C. The figure also indicates the ΔH_{ion} values for the different buffers used in these experiments.

pH Dependence of ΔH_{obs} *as a Function of* ΔH_{ion}. One major advantage of using ITC is that it provides a direct measure of the 'observed' change of enthalpy of an interaction (ΔH_{obs}). The data based on the ΔH_{obs} of binding can be used independently to validate the model adopted to fit the data for the pH dependence of K_{obs}. Since there is a change in the number of protons taken up or released by the buffer in forming the complex, the measured ΔH_{obs} has a component term arising from $z(N)$. ΔH_{obs} can be defined by eq 3:

$$\Delta H_{obs} = \Delta H_0 + z(N)\Delta H_{ion} \qquad (3)$$

where ΔH_{ion} is the ionization enthalpy of the buffer, ΔH_0 is the binding enthalpy that would be measured if ΔH_{ion} was equal to zero, and $z(N)$ is the number of groups with identical pK_a's protonated on going from the free to the bound state at a given pH. The change in the number of protons associated with the interacting molecules at a given pH can be determined by measuring ΔH_{obs} as a function of the ionization enthalpy (ΔH_{ion}) of the buffer (*25*−*31*). This was achieved by performing a series of experiments in a range of different buffer types. A possible difficulty with this approach is that different buffer components could potentially interact with the protein and hence give rise to bigger differences in the intrinsic thermodynamic parameters than would be expected. This was not observed since, under similar conditions, ΔG was essentially invariant at each pH regardless of which buffer was used (Table 1).

Examination of Table 1 shows that the ΔH_{obs} varies as a function of both pH and buffer type used. The dependence of ΔH_{obs} on ΔH_{ion} in Figure 5 provides a direct measure of

Table 2: Calorimetrically Measured Thermodynamic Parameters for the *Mun*I−SP Interaction as a Function of Buffer Type and Temperature[a]

buffer[b]	[NaCl] mM	pH	T (°C)	ΔH_{obs}[b] (kJ mol^{-1})	K_{obs}[b] ($\times 10^5$ M^{-1})	n[b]	ΔG_{obs}[c] (kJ mol^{-1})	$T\Delta S$ (kJ mol^{-1} K^{-1})
MES[d]	200	6.5	13.7	−46.5 ± 1.2	11.5 ± 0.2	0.9	−33.3	−13.2
MES	200	6.5	19.5	−63.7 ± 1.2	12.6 ± 0.1	1.1	−34.2	−29.5
MES	200	6.5	25.2	−81.2 ± 1.7	12.5 ± 0.1	1.1	−34.8	−46.4
MES	200	6.5	30.2	−89.3 ± 1.2	17.9 ± 0.2	1.2	−36.3	−53.0
MOPS[e]	200	7.5	13.2	−36.5 ± 1.3	5.5 ± 0.5	1.1	−31.5	−5.0
MOPS	200	7.5	16.9	−42.8 ± 1.2	7.5 ± 0.6	0.9	−32.6	−10.2
MOPS	200	7.5	23.1	−54.5 ± 1.2	6.5 ± 0.5	0.9	−32.9	−21.6
MOPS	200	7.5	30.1	−70.7 ± 1.5	5.1 ± 0.5	0.9	−33.2	−37.5
TAPS[f]	200	8.5	9.1	+4.8 ± 1.6	2.8 ± 0.2	0.95	−29.4	+34.2
TAPS	200	8.5	15.1	−7.0 ± 1.4	2.1 ± 0.1	0.91	−29.4	+22.4
TAPS	200	8.5	22.0	−19.4 ± 1.5	2.7 ± 0.2	0.91	−30.7	+11.3
TAPS	200	8.5	30.0	−31.6 ± 3	3.2 ± 0.3	0.91	−31.9	+0.3

[a] All binding data reported are based on at least two individual ITC experiments. [b] For key to superscripts, see Table 1. [c] Heat capacity determined from the slope of linear least-squares fitting of the temperature-dependent enthalpy data shown in Figure 7. [d] $\Delta C_p = -2.7 \pm 0.3$ kJ mol^{-1} K^{-1} in MES buffer. [e] $\Delta C_p = -2.1 \pm 0.2$ kJ mol^{-1} K^{-1} in MOPS buffer. [f] $\Delta C_p = -1.7 \pm 0.1$ kJ mol^{-1} K^{-1} in TAPS buffer.

the number of protons exchanged during binding at each pH. Linear least-squares fits of the data of the binding of *Mun*I to the SP oligonucleotide are shown to be accompanied by an uptake of 1.2, 1.5, 0.6, 0.7, and 2.6 protons at pH values of 5.75, 6.5, 7.5, 8.0, and 8.5, respectively (for clarity, data sets at three pH values only are shown in Figure 5). All of the $z(N)$ values are positive, indicating that at all of the pH values studied there are more protons associated with the complex than in the free interacting molecules; i.e., protons are sequestered into the structure on binding.

The Different pH Change in Heat Capacity (ΔC_p) Shows Significant Variation. ITC was used to examine the temperature dependence of the binding enthalpy for the *Mun*I−SP interaction at three different pH values (Table 2). Figure 6 shows the relationship between binding enthalpy (ΔH) and temperature at pH values 6.5, 7.5, and 8.5. The slope of a linear least-squares fit of these data yields the binding-induced heat capacity change for the process, $\Delta C_p = -2.7$, -2.1, and -1.7 kJ mol^{-1} K^{-1} at pH values 6.5, 7.5, and 8.5, respectively. Figure 6 also shows the effect of temperature on the entropy term, $T\Delta S$. At the three pH values studied, the ΔG is independent of temperature. The insensitivity of ΔG to temperature is due to compensation of temperature-dependent enthalpy and entropy terms in common with many other protein−DNA systems (*23*).

Correlation of $\Delta C_{p,obs}$ with Surface Area Burial on Complex Formation. The correlation of the ΔC_p with the burial of surface area of the interacting components on forming a complex interface has been demonstrated for a number of systems (*20*). In this work, we observe large changes in ΔC_p at different pH values. Thus, assuming that the interacting molecules do not possess significant conformational differences in the free state and on complex formation at the three pH values investigated, this correlation is sensitive to protonation events occurring on complex formation.

There are currently no reported solution or crystal structures for wild-type *Mun*I, the SP oligonucleotide, or the complex of the two; thus, in order to estimate changes in surface area burial upon binding for the formation of the wild-type *Mun*I−SP complex, we have used the crystal structure of a D83A *Mun*I mutant−SP complex (*18*). The surface area calculations determined from the D83A *Mun*I−SP complex show that the binding of protein to DNA results

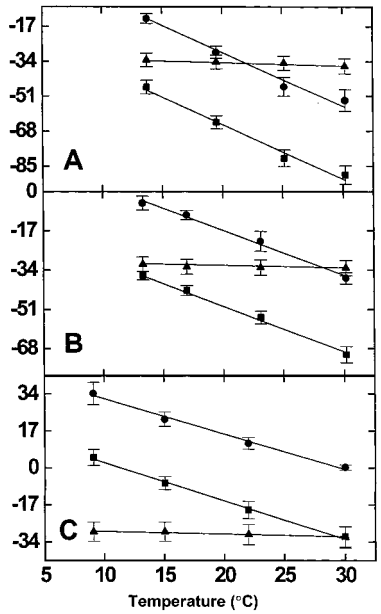

FIGURE 6: Heat capacity plots for the interaction of SP oligonucleotide with *Mun*I. This figure shows the temperature dependence of ΔH_{obs} (squares), ΔG_{obs} (triangles), and $T\Delta S_{obs}$ (circles) for the SP−*Mun*I interaction. All experiments were carried out in buffers containing 200 mM NaCl and 1 mM Na_2EDTA; in panel A, 10 mM MES, pH 6.5, was used, and in panels B and C, 10 mM MOPS, pH 7.5, and 10 mM TAPS, pH 8.5, were used, respectively. Linear least-squares fitting of the temperature-dependent enthalpy data gave $\Delta C_{p,obs}$ values of -2.7 ± 0.3 at pH 6.5, -2.1 ± 0.2 at pH 7.5, and 1.7 ± 0.1 kJ mol^{-1} K^{-1} at pH 8.5.

in a modest ~15% loss of solvent-accessible surface relative to the separated components. Table 3 shows a summary of the calculated surface areas. These data show that ~51% of surface buried from exposure to solvent for this interaction is polar rather than hydrophobic. A predicted change in the heat capacity value can be calculated using the data in Table 3 and an empirical relationship (*20*) (see Materials and Methods). Using this relationship, a ΔC_p of -1.15 ± 0.39 kJ mol^{-1} K^{-1} is predicted for the *Mun*I dimer. Thus, there is a discrepancy of 1.55 kJ mol^{-1} K^{-1} at pH 6.5 to 0.55 kJ mol^{-1} K^{-1} at pH 8.5 between the calculated and the experimentally determined change in heat capacity on complex formation. Such discrepancies have been reported for a number of protein−DNA complexes (*13, 31, 32*). There

Table 3: Computed SASA Burial for the 1:1 *Mun*I(Dimer)−d(GCCAATTGGC)$_2$ Complex

	solvent-accessible surface area (Å^2)[a]		
structure	nonpolar SASA (A_{np})	polar SASA (A_p)	total SASA (A)
*Mun*I(dimer)−DNA complex[b]	11388.070	7472.160	18860.230
bound *Mun*I protein	10781.910	7290.170	18072.080
bound DNA	2169.276	1930.231	4099.507
canonical DNA[c]			
A-DNA duplex	2052.424	1822.971	3875.395
B-DNA duplex	2199.722	1859.337	4059.059
induced changes[d]	ΔA_{np} = −1593.562 (−1563.116)	ΔA_p = −1677.347 (−1748.241)	ΔA = −3270.909 (−3311.356)
calculated ΔC_p[e]	−1.15 ± 0.39 (or −1.07 ± 0.39)		

[a] Solvent-accessible surface areas determined for all-atom coordinate sets (i.e., including all H-atoms) using the GRASP 1.3.6 program (*19*), at the highest possible definition and with a spherical probe of 1.4 Å radius. [b] From reported crystal structure for the 1:1 *Mun*I(dimer)−DNA complex [(*18*); PDB entry: 1D02; NDB entry: pd0151]. [c] Canonical A- and B-type DNA 10-mer duplexes of this sequence generated using the GENHELIX-2 program (T. C. Jenkins, unpublished data). [d] Binding-induced alterations in the SASA terms calculated using: $\Delta A = \Delta A_{np} + \Delta A_{np}$, where $\Delta A_{np} = A_{np}(\text{complex}) - [A_{np}(\text{protein}) + A_{np}(\text{DNA})]$ and $\Delta A_p = A_p(\text{complex}) - [A_p(\text{protein}) + A_p(\text{DNA})]$. The canonical B-DNA structure was assumed for the native DNA; values in parentheses were calculated for the protein-bound DNA molecule. [e] Heat capacity changes calculated using the empirical relationship: ΔC_p (cal mol^{-1} K^{-1}) = 0.32(±0.04)·ΔA_{np} − 0.14(±0.04)·ΔA_p, where A_{np} and A_p are in Å^2 units, respectively (*20, 37*). Note that the ΔC_p values for each DNA were calculated using area terms for the protein taken from its DNA-bound complex rather than for any deposited native coordinates.

are several potential contributions to change in heat capacity, which are not included in the empirical calculation of surface area (*33, 34*). Quite clearly, in this work the effect of a number of protonation events impinges on the observed value of $\Delta C_{p,obs}$.

DISCUSSION

Here we present ITC data for the formation of a complex between *Mun*I and DNA. From these data, it is clear that recognition of a specific DNA sequence has very different features than that of a nonspecific sequence. The nonspecific interaction is accompanied by a small enthalpic contribution, and a negligible ΔC_p. This phenomenon seems to be a general characteristic of protein−DNA interactions. The ITC data derived for the interaction over the pH range of 3.5 units show that protonation plays an important role in binding. Indeed, the K_{obs} increases by about 20-fold on decreasing the pH from 9.0 to 5.5 (Table 1). Using a model derived from data-fitting to the pH dependence of the observed equilibrium binding constant, we suggest that protonation occurs on moieties which undergo pK_a shifts in two distinct ranges (from 6.0 in the free form to 6.9 in the complex and from 8.9 in the free form to approximately 10 in the complex). The effect of pH on the K_{obs} was significantly more pronounced at the low pH range, implying a stronger proton linkage. Our data also suggest that more than one protonation event occurs in each pK_a range. This would be consistent with at least one protonation per *Mun*I molecule in the dimer contributing to the observed effect.

The unequivocal identification of the moieties which undergo protonation in these ranges is not possible from the data reported herein alone. Active site carboxylates provide potential candidates for the protonated groups in the lower pH range. The pK_a's of these residues have not been experimentally determined. ^{25}Mg-NMR titration experiments on the *Pvu*II restriction enzyme, however, demonstrated that two active site carboxylate residues in the bound form had pK_a values of 6.7 (*35*). Comparison of the cocrystal structure of the D83A mutant of *Mun*I (*18*) with that of *Pvu*II (*36*) shows that the D83 and E98 residues of *Mun*I are in similar positions to their counterparts with the anomalous pK_a values in *Pvu*II. Biochemical studies, accompanied by site-directed mutational analysis (*8, 9*), suggested that a carboxylate residue(s) with an anomalous pK_a in the range 6.5−8.0 in the bound state control(s) DNA binding specificity of *Mun*I in the absence of Mg^{2+} ions. The pK_a value of 6.9 reported here is within this range, but slightly higher than that reported for *Pvu*II. It is, however, highly probable that bringing one of the phosphate oxygens of the scissile phosphate to the vicinity of the active site causes a further increase of the pK_a. In principle, two carboxylate residues and a phosphate oxygen at the active site in the *Mun*I−DNA complex might represent a conjugated system of three negative charges. The uptake of protons by each protein molecule in the lower pH range might be required for stabilization of this system. It is, thus, tempting to speculate that sequestering of the divalent Mg^{2+} ion by this negative site might also impose a similar level of stability. This hypothesis is further supported by data from kinetic studies which indicated that protons and Mg^{2+} ions compete for binding at the active site of *Mun*I (*17*). At high pH, there is a large shift of the pK_a of the ionizable groups for free and bound from 8.9 to approximately 10, respectively. These values are less precise due to the smaller changes in K_{obs} at high pH (see Figure 3). The likely groups involved in protonation in this range are cysteine residues or the oligonucleotide bases. It is interesting to note the presence of a cysteine residue located in a helix of the *Mun*I structure proximal to the sugar−phosphate backbone in the major groove of the DNA. It is anticipated that a similar binding study in which potential ionizable groups are replaced using site-directed mutagenesis will reveal the identity of the residues invoked in this work.

REFERENCES

1. Roberts, R. J., and Halford, S. E. (1993) Type II restriction endonucleases. in *Nucleases* (Linn, S. M., Lloyd, R. S., and Roberts, R. J., Eds.) 2nd ed., pp 35−88, Cold Spring Harbor Laboratory Press, Cold Spring Harbor, NY.
2. Terry, B. J., Jack, W. E., Rubin, R. A., and Modrich, P. (1983) Thermodynamic parameters governing interactions of *Eco*RI endonuclease with specific and nonspecific DNA sequences. *J. Biol. Chem. 258*, 9820−9825.
3. Aiken, C. R., Fischer, E. W., and Gumport, R. I. (1991) The specific binding, bending and unwinding of DNA by *Rsr*I endonuclease, an isoschizomer of *Eco*RI endonuclease. *J. Biol. Chem. 266*, 19063−19069.
4. Xu, S. Y., and Schildkraut, I. (1991) Isolation of *Bam*HI variants with reduced cleavage activities. *J. Biol. Chem. 266*, 4425−4429.
5. Taylor, J. D., Badcoe, I. G., Clarke, A. R., and Halford, S. E. (1991) *Eco*RV restriction endonuclease binds all DNA sequences with equal affinity. *Biochemistry 30*, 8743−8753.
6. Zebala, J. A., Choi, J., and Barany, F. (1992) Characterization of steady state, single-turnover and binding kinetics of the *Taq*I

restriction endonuclease. *J. Biol. Chem. 267*, 8097−8105.
7. Siksnys, V., and Pleckaityte, M. (1993) Catalytic and binding properties of restriction endonuclease *Cfr*9I. *Eur. J. Biochem. 217*, 411−419.
8. Lagunavicius, A., Grazulis, S., Balciunaite, E., Vainius, D., and Siksnys, V. (1997) DNA binding specificity of *Mun*I restriction endonuclease is controlled by pH and calcium ions: involvement of active site carboxylate residues. *Biochemistry 36*, 11093−11099.
9. Lagunavicius, A., and Siksnys, V. (1997) Site-directed mutagenesis of putative active site residues of *Mun*I restriction endonuclease: replacement of catalytically essential carboxylate residues triggers DNA binding specificity. *Biochemistry 36*, 11086−11092.
10. Stakenas, P. S., Zaretskaya, N. M., Maneliene, Z. P., Mauricas, M. M., Butkus, V., and Yanulaitis, A. A. (1992) *Mun*I mycoplasmic restriction modification system and its possible role in pathogenesis. *Mol. Biol. 26* (3), 417−426.
11. Puglisis, J. D., and Tinoco, I., Jr. (1989) Absorbance melting curves of RNA. *Methods Enzymol. 180*, 304−325.
12. Wiseman, T., Williston, S., Brandts, J. F., and Lin, L.-N. (1989) Rapid measurement of binding constants and heats of binding using a new titration calorimeter. *Anal. Biochem. 179*, 131−137.
13. Ladbury, J. E. (1995) Counting the calories to stay in the groove. *Structure 3*, 635−639.
14. Haq, I., Jenkins, T. C., Chowdhry, B. Z., Ren, J., and Chaires, J. B. Parsing the free energy of drug−DNA interactions. *Methods Enzymol. 323*, 373−405.
15. Ellis, K. J., and Morrison, J. F. (1982) Buffers of constant ionic strength for studying pH-dependent processes. *Methods Enzymol. 87*, 405−426.
16. Christensen, J. J., Hansen, L. D., and Izatt, R. M. (1976) Handbook of ionization heats and related thermodynamic quantities, John Wiley and Sons, New York.
17. Sasnauskas, G., Jeltsch, A., Pingoud, A., and Siksnys, V. (1999) Plasmid DNA cleavage by *Mun*I restriction enzyme: single-turnover and steady-state kinetic analysis. *Biochemistry 38* (13), 4028−4036.
18. Deibert, M., Grazulis, S., Janulaitis, A., Siksnys, V., and Huber, R. (1999) Crystal structure of *Mun*I restriction endonuclease in complex with cognate DNA at 1.7 Å resolution. *EMBO J. 18*, 5805−5816.
19. Nicholls, A., Sharp, K., and Honig, B. (1991) Protein folding and association: insights from the interfacial and thermodynamic properties of hydrocarbons. *Proteins: Struct., Funct., Genet. 11*, 281−296.
20. Spolar, R. S., and Record, M. T. (1994) Coupling of local folding to site-specific binding of proteins to DNA. *Science 263*, 777−783.
21. Takeda, Y., Ross, P. D., and Mudd, C. P. (1992) Thermodynamics of Cro-protein−DNA interactions. *Proc. Natl. Acad. Sci. U.S.A. 89*, 8180−8184.
22. Ladbury, J. E., Wright, J. G., Sturtevant, J. M., and Sigler, P. B. (1994) A thermodynamic study of the *trp* repressor-operator interaction. *J. Mol. Biol. 238*, 669−681.
23. Jen-Jacobson, L., Engler, L. E., Ames, J. T., Kurpiewski, M. R., and Grigorescu, A. (2001) *Supramol. Chem. 12*, 143−160.
24. Wyman, J., and Gill, S. J. (1990) Binding and Linkage: The Functional Chemistry of Biological Macromolecules. University Science Books, Mill Valley, CA.
25. Baker, B. M., and Murphy, K. P. (1996) Evaluation of linked protonation effects in protein binding reactions using isothermal titration calorimetry. *Biophys. J. 71*, 2049−2055.
26. Bradshaw, J. M., and Waksman, G. (1998) Calorimetric investigation of proton linkage by monitoring both the enthalpy and association constant of binding: application to the interaction of the Src SH2 domain with a high-affinity tyrosyl phosphate. *Biochemistry 37*, 15400−15407.
27. Eftink, M. R., Anusiem, A. C., and Biltonen, R. L. (1983) Enthalpy−entropy compensation and heat capacity changes for protein ligand interactions: general thermodynamic models and data for the binding of nucleotides to ribonuclease A. *Biochemistry 22*, 3884−3896.
28. Takahashi, K., and Fukada, H. (1985) Calorimetric studies of the binding of *Streptomyces* subtilisin inhibitor to subtilisin of *Bacillus subtilis* strain N′. *Biochemistry 24*, 297−300.
29. Murphy, K. P., Xie, D., Garcia, K. C., Amzel, L. M., and Freire, E. (1993) Structural energetics of peptide recognition: angiotensin II/antibody binding. *Proteins: Struct., Funct., Genet. 15*, 113−120.
30. Kresheck, G. C., Vitello, L. B., and Erman, J. E. (1995) Calorimetric studies on the interaction of the horse ferricytochrome *c* and yeast cytochrome *c* peroxidase. *Biochemistry 34*, 8398−8405.
31. Gomez, J., and Freire, E. (1995) Thermodynamic mapping of the inhibitor site of the aspartic protease endothiapepsin. *J. Mol. Biol. 252*, 337−350.
32. Hyre, D. E., and Spicer, L. D. (1995) Thermodynamic evaluation of binding interactions in the methionine repressor system of *Escherichia coli* using isothermal titration calorimetry. *Biochemistry 34*, 3212−3221.
33. Morton, C. J., and Ladbury, J. E. (1996) Water-mediated protein−DNA interactions: the relationship of thermodynamics to structural detail. *Prot. Sci. 5*, 2115−2113.
34. Sturtevant, J. M. (1977) Heat capacity and entropy changes in processes involving proteins. *Proc. Natl. Acad. Sci. U.S.A. 74*, 2236−2240.
35. Dupureur, C. M., and Conlan, L. H. (2000) A catalytically deficient active site variant of *Pvu*II endonuclease binds Mg(II) ions. *Biochemistry 39*, 10921−10927.
36. Cheng, X. D., Balendiran, K., Schildkraut, I., and Anderson, J. E. (1994) Structure of *Pvu*II endonuclease with cognate DNA. *EMBO J. 13*, 3927−3935.
37. Record, M. T., Jr., Ha, J.-H., and Fisher, M. A. (1991) Analysis of equilibrium and kinetic measurement to determine thermodynamic origins of stability and specificity and mechanism of formation of site-specific complexes between proteins and helical DNA. *Methods Enzymol. 208*, 291−343.

BI0113566